Analyzing IEEE 802.11g and IEEE 802.16e Technologies for Single-hop Inter-vehicle Communications

Raúl Aquino-Santos[1], Victor Rangel-Licea[2], Aldo Mendez[3], Arthur Edwards[1], Miguel A. Garcia-Ruiz[1], Eduardo Flores[1].

[1]Faculty of Telematics, University of Colima, Av. Universidad 333, C. P. 28045, Colima, Colima, México.
[2]Department of Telecommunications, National Autonomous University of México, Mexico, D.F.
[3]Universidad Autónoma de Tamaulipas, Carretera Reynosa-San Fernando, cruce con canal Rodhe, Reynosa Tamaulipas, México.

Abstract. - This chapter analyzes two prominent technologies, IEEE 802.11g (WiFi) and IEEE 802.16e (WiMAX), for single-hop inter-vehicular communications. We begin our analysis by comparing the physical and MAC layers of both standards. Following this, we simulate two scenarios, one with IEEE 802.11g and the other with IEEE 802.16e, in a single-hop inter-vehicular communication network (SIVC). In both scenarios, the Location-Based Routing Algorithm with Cluster-Based Flooding (LORA-CBF) was employed to create a hierarchical vehicular organization that acts as a cluster-head with its corresponding member nodes. The simulation scenarios consist of five different node sizes of 20, 40, 60, 80 and 100 vehicles, respectively. We propose a novel simulation model that is suitable for mesh topologies in WiMAX networks and provide preliminary results in terms of delay, load and throughput for single-hop inter-vehicle communication.

Keyword: IEEE 802.11g, IEEE 802.16e, VANETs, Single-hop inter-vehicular communications, mesh topology, LORA-CBF.

1. INTRODUCTION

Interest in inter-vehicular and vehicle-to-roadside communication has significantly increased over the last decade, in part, because of the proliferation of wireless networks. Most research in this area has concentrated on vehicle-to-roadside communication, also called beacon-vehicle communication in which vehicles share the medium by accessing different time slots.
Some applications for vehicle-to-roadside communication, including Automatic Payment, Route Guidance, Cooperative Driving, and Parking Management have been developed to function within limited communication zones of less than 60 meters. However, the IEEE 802.11 Standard has led to increased research in the areas of wireless ad hoc networks and location-

based routing algorithms, (Morris et. al., 2000), (Da Chen, Kung, & Vlah, 2001), (Füßler, et. al., 2003), (Lochert, et. al., 2003), (Kosh, Schwingenschlögl, & Ai, 2002). Applications for inter-vehicular communication include Intelligent Cruise Control, Intelligent Maneuvering Control, Lane Access, and Emergency Warning, among others. In (Morris et. al., 2000), the authors propose using Grid (Li, et. al., 2000), a geographic forwarding and scalable distributed location service, to route packets from car to car without flooding the network. The authors in (Da Chen, Kung, & Vlah, 2001) propose relaying messages in low traffic densities, based on a microscopic traffic simulator that produces accurate movement traces of vehicles traveling on a highway, and a network simulator to model the exchange of messages among the vehicles. Da Chen et. al., employ a straight bidirectional highway segment of one or more lanes. The messages are propagated greedily each time step by hopping to the neighbor closest to the destination. The authors in (Füßler, et. al., 2003), compare a topology-based approach and a location-based routing scheme. The authors chose GPSR (Karp & Kung, 2000) as the location-based routing scheme and DSR (Johnson, Maltz, & Hu, 2007) as the topology-based approach. The simulator used in (Füßler, et. al., 2003) is called FARSI, which is a macroscopic traffic model. In (Lochert, et. al., 2003), the authors compare two topology-based routing approaches, DSR and AODV (Perkins, Belding-Royer & Das, 2003), versus one position-based routing scheme, GPSR, in an urban environment. Finally, in (Kosh, Schwingenschlögl, & Ai, 2002), the authors employ a geocast routing protocol that is based on AODV.

In inter-vehicular communication, vehicles are equipped with on-board computers that function as nodes in a wireless network, allowing them to contact other similarity equipped vehicles in their vicinity. By exchanging information, vehicles can obtain information about local traffic conditions, which improves traffic control, lowers contamination caused by traffic jams and provides greater driver safety and comfort.
Future developments in automobile manufacturing will also include new communication, educational and entertainment technologies. The major goals are to provide increased automotive safety, achieve smoother traffic flow, and improve passenger convenience by providing information and entertainment. In order to avoid communication costs and guarantee the low delays required to exchange safety-related data between cars, inter-vehicular communication (IVC) systems, based on wireless ad hoc networks, represent a promising solution for future road communication scenarios. IVC allows vehicles to organize themselves locally in ad hoc networks without any pre-installed infrastructure. Communication in future IVC systems will not be restricted to neighboring vehicles traveling within a specific radio transmission range. As in typical wireless scenarios, the IVC system will provide multi-hop communication capabilities by using “relay” vehicles that are traveling between the sender and receiver. Vehicles between the source-destination act as intermediate vehicles, relaying data to the receiver. As a result, the multi-hop capability of the IVC system significantly increases the virtual communication range, as it enables communication with more distant vehicles.

1.1 ORIGINS OF AD HOC WIRELESS NETWORKS

Historically, mobile ad-hoc networks have primarily been used for tactical network-related applications to improve battlefield communications and survivability. The dynamic nature of military applications means it is not always possible to rely on access to a fixed pre-placed communication infrastructure on the battlefield. The Packet Radio Network (PRNET), under the sponsorship of the Defense Advanced Research Project Agency (DARPA), is considered the precursor of mobile wireless ad-hoc networks (MANET) (Toh, 2002).
PRNET was the first implementation of ad-hoc wireless networks with mobile nodes. This was primarily inspired by the efficiency of packet switching technology, such as bandwidth sharing and store-and-forward routing and its possible applications in mobile wireless environments.
Survivable Radio Networks (SURANs) were deployed by DARPA in 1983 to address open issues in PRNET in the areas of network scalability, security, processing capability, and energy management. The main objectives of these efforts was to develop network algorithms to support networks that can scale to tens of thousands of nodes and can resist security attacks, as well as use small, low cost, low-power radio technology that can support more sophisticated packet

radio protocols. This effort resulted in the design of Low-cost Packet Radio (LPR) technology in 1987, which featured a digitally controlled DS spread spectrum radio with an integrated Intel 8086 microprocessor-based packet switch.

Although early MANET application and deployments were military oriented, non-military applications have grown substantially since then and have become the main focus today. This has been the case the last few years due to rapid advances in mobile ad-hoc networking research. Mobile ad-hoc networks have attracted considerable attention and interest from the commercial sector as well as the standards community. The introduction of new technologies such as IEEE 802.11g and IEEE 802.16e greatly facilitate the deployment of ad-hoc technology outside of the military domain. As a result, many new ad-hoc networking applications have since been conceived to help enable new commercial and personal communication beyond the tactical networks domain, including personal area networking, home networking, law enforcement operations, search-and-rescue operations, commercial and educational applications, sensor networks, and so on.

1.2 INTRODUCTION TO WIRELESS NETWORKS

The requirements of data communication, beyond the physical link, has resulted in the need for wireless networks, which have been fuelled by fabrication improvements of digital and RF circuits, new large-scale circuit integration, and other miniaturization technologies that make portable radio equipment smaller, cheaper, and more reliable.

Wireless Networks (WNs) represent flexible data communications systems that can be implemented as an extension to, or as an alternative for, a wired LAN. Using a form of electromagnetic radiation as the network medium, most commonly in the form of radio waves, wireless LANs transmit and receive data over air, minimizing the need for wired connections (cables). Thus, WNs combine data connectivity with user mobility. By combining mobile devices with wireless communications technologies, the vision of being connected at anytime and anywhere will soon become a reality.

Whereas today's expensive wireless infrastructure depends on centrally deployed hub and one-hop stations, mobile ad hoc networks consist of nodes that are autonomously self-organize into networks. In ad-hoc networks, the nodes themselves and their intercommunicability comprise the network. This advantage permits seamless low cost communication in a self-organized fashion that can be easily deployed. The large degree of freedom and self-organizing capabilities of ad-hoc networks make them different from other networking solutions. For the first time, individuals have the opportunity to create their own networks, which can be deployed easily and inexpensively within the specified area determined by the specific needs and characteristics established by the user.

Ad-hoc networks represent a key step in the evolution of wireless networks. However, they inherit many of the traditional problems of wireless and mobile communications such as bandwidth optimization, power control and transmission quality enhancements. There are presently two standards that can be applied to single-hop inter-vehicular communications: IEEE 802.11g, and IEEE 802.16e.

1.2.1 IEEE 802.11 WLAN ARCHITECTURE

The IEEE 802.11 was the first international standard for WLANs (O'Hara, & Petrick, 1999). The basic service set (BSS) is the fundamental building block of the IEEE 802.11 architecture. A BSS is defined as a group of stations that are under the direct control of a single coordination function (e.g. Direct Coordination Function (DCF) or Point Coordination Function (PCF)), which is defined below.

The geographical area covered by the BSS is known as the Basic Service Area (BSA), which is analogous to a cell in a cellular communication network. Conceptually, all stations in a BSS can communicate directly with all other stations in a BSS.

An ad-hoc network is a defined group of stations that are organized into a single BSS for the purposes of inter-networked communications, without the aid of any additional network

infrastructure. Figure 1 provides an illustration of a wireless infrastructure and independent BSS. The IEEE 802.11 Standard defines an ad-hoc network as an independent BSS.

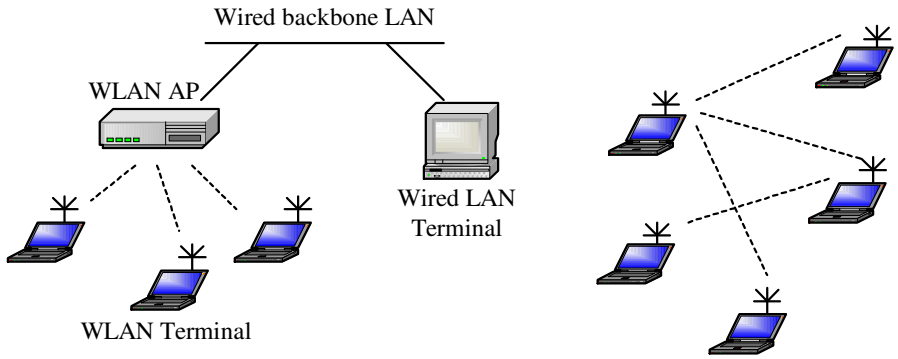

Figure 1: Basic WLAN Architectures: Infrastructure and Ad-hoc.

Any station can establish a direct communication session with any other station in the BSS in an ad-hoc network, without having to channel all traffic through a centralized access point (AP).

Physical Layer

The IEEE specification calls for three different physical-layer implementations: Frequency Hopping Spread Spectrum (FHSS), Direct Sequence Spread Spectrum (DSSS), and Infrared. The FHSS utilizes the 2.4 GHz Industrial, Scientific, and Medical (ISM) band (e.g. 2.4- 2.4835 GHz). In the United States, a maximum of 79 channels are specified in the hopping set. The first channel has a central frequency of 2.402 GHz, and all subsequent channels are spaced at 1 MHz intervals. The 1 MHz separation is mandated by the FCC for the 2.4 GHz ISM band. The channel separation corresponds to 1 Mb/s of instantaneous bandwidth. Three different hopping sequence sets are established with 26 hopping sequences per set. Different hopping sequences enable multiple BSSs to coexist in the same geographical area, which may become necessary to alleviate congestion and maximize the total throughput of a single BSS. The minimum hop rate permitted is 2.5 hops/seconds. The basic access rate of 1 Mb/s uses two-level Gaussian frequency shift keying (GFSK). The enhanced access rate of 2 Mb/s uses four-level GFSK (Figure 2). The DSSS also uses the 2.4 GHz ISM frequency band, where the 1 Mb/s basic rate is encoded using differential binary phase shift keying (DBPSK), and a 2 Mb/s enhanced rate uses differential quadrature phase shift keying (DQPSK). The spreading is done by dividing the available bandwidth into 11 sub-channels, each 11 MHz wide, and using an 11-chip Barker sequence to spread each data symbol. The maximum channel capacity is therefore (11 chips/symbol)/ (11 MHz) = 1 Mb/s if DBPSK is used.

In October 1997, the IEEE 802 Executive Committee approved two extensions for higher data rate transmissions. The first extension, IEEE 802.11a, defines requirements for a PHY layer operating in the 5.0 GHz frequency and data rate transmission ranging from 6 Mbps to 54 Mbps. The second extension, IEEE 802.11b, defines a set of PHY layer specifications operating in the 2.4 GHz frequency band up to 11 Mbps. Both PHY layers are designed to operate with the existing MAC layer.

The IEEE 802.11a PHY is one of the physical layer extensions of IEEE 802.11 and is referred to as orthogonal frequency division multiplexing (OFDM) and the IEEE 802.11b is referred to as high rate direct sequence spread spectrum (HR/DSSS). The HR/DSSS PHY provides two functions. First, the HR/DSSS extends the PSDU data rates to 5.5 and 11 Mbps using an enhanced modulation technique, called Complementary Code Keying (CCK). Secondly, the HR/DSSS PHY provides a rate shift mechanism, which allows 11 Mbps networks to fall back to 1 and 2 Mbps and interoperates with the legacy IEEE 802.11 standard. The most recent

commercial standard is IEEE 802.11g, approved in June 2003, which we use in our simulation. The IEEE 802.11g standard provides optional data rates transmission of up to 54 Mbps, and requires compatibility with 802.11b devices to protect the substantial investments in today's WLAN installations. The 802.11g standard includes mandatory and optional components. It specifies OFDM and CCK as the mandatory modulation schemes with 24 Mbps as the maximum mandatory data rates, but it also provides for optional higher data rates of 36, 48 and 54 Mbps.

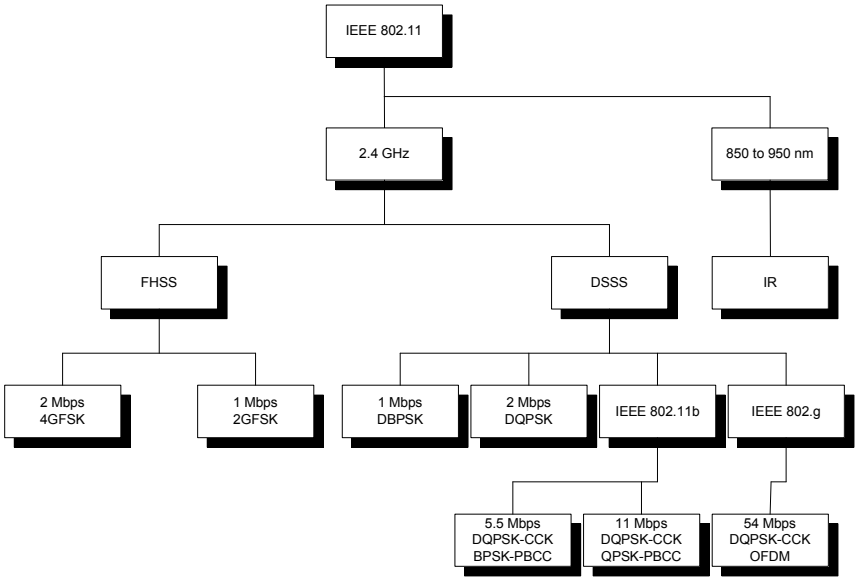

Figure 2: IEEE 802.11 Architecture.

Medium Access Control Sub-layer

The MAC sub-layer is responsible for channel allocation procedures, protocol data unit (PDU) addressing, frame formatting, error checking, and data fragmentation and reassembly.
The transmission medium can operate in the contention mode exclusively, requiring all stations to contend for access to the channel for each packet transmitted. The medium can also alternate between the contention mode, known as the contention period (CP) under the Distribute Coordination Function (DCF), and a contention-free period (CFP) under the Point Coordination Function (PCF). During the CFP, medium usage is controlled (or mediated) by the AP, thereby eliminating the need for stations to contend for channel access.
The DCF is the fundamental access method used to support asynchronous data transfer on a best effort basis. The DCF operates exclusively in ad-hoc networks and is based on carrier sense multiple access with collision avoidance (CSMA/CA). In IEEE 802.11, carrier sensing is performed at both the air interface, referred to as physical carrier sensing and at the MAC sub-layer, also called virtual carrier sensing. Physical carrier sensing detects the presence of other IEEE 802.11 WLAN users by analyzing all detected packets and also detecting activity in the channel via relative signal strength from other sources.
A source station performs virtual carrier sensing by sending MPDU duration information in the header of request to send (RTS), clear to send (CTS), and data frames. The duration field indicates the amount of time (in microseconds) after the end of the present frame. The channel will then be utilized to complete the successful transmission of the data or management frame. Stations in the BSS use the information in the duration field to adjust their network allocation vector (NAV), which indicates the amount of time that must elapse to complete a transmission session before the channel can be sampled again for idle status. The channel is marked busy if either the physical or virtual carrier sensing mechanisms indicates the channel is busy.

On the other hand, the PCF is an optional capability, which is connection-oriented, and provides contention-free (CF) frame transfer. The PCF relies on the point coordinator (PC) to perform polling, enabling polled stations to transmit without contending for the channel. The function of the PC is performed by the AP within each BSS.

1.2.2 PHYSICAL LAYER OF 802.11G

The 802.11g physical (PHY) layer supports 4 modulation schemes (Vassis et al., 2005). Two of these schemes, ERP-OFDM and ERP-CCK/DSSS, are mandatory and two, ERP-PBCC and DSSS-OFDM, are optional. Of the four schemes, only ERP-OFDM and DSSS-OFDM provide data rates of up to 54Mb/s using OFDM modulation schemes, while also providing explicit support for interoperating with 802.11b nodes. Such support is necessary as 802.11b nodes cannot detect or interpret OFDM modulated signals.

The ERP-OFDM scheme is a variant of the 802.11a PHY scheme modified for use in the 2.4 GHz band (Szczypiorski, and Lubacz, 2008). In this mode, all the data is sent by OFDM and can only be received by 802.11g stations. It is therefore known as 802.11g-only mode. The data rates are also 6, 9, 12, 18, 24, 36, 48, and 54 Mbps.

The ERP-CCK mode is used for compatibility with 802.11b stations. CCK stands for Complementary Code Keying; the data rates supported are 5.5 and 11Mbit/s.

In the ERP-DSSS mode, data is transmitted using a technique called Direct Sequence Spread Spectrum (DSSS). ERP-DSSS provides backward compatibility with 802.11 stations supporting data rates of 1 and 2Mbit/s.

The ERP-PBCC mode is optional and rarely used. PBCC, or Packet Binary Convolutional Coding, is used in conjunction with DSSS. The data rates achieved by ERP-PBCC are 5.5, 11, 22, and 33Mbit/s.

The DSSS-OFDM scheme is a hybrid modulation scheme that combines a DSSS and OFDM. DSSS is employed to transmit the header of a PHY frame. Doing so allows 802.11b devices to receive information and update their NAVs dynamically. Therefore, 802.11b stations and 802.11g stations can be operated in the same network. The actual data is OFDM modulated and cannot be received by 802.11b stations. The data rates are 6, 9, 12, 18, 24, 36, 48, and 54Mbit/s.

1.2.3 PHY FRAMES

In order to transmit packets over the wireless link, the MAC frames are encapsulated into PHY frames. The format of the transmitted PHY Protocol Data Unit (PPDU) consists of a PLCP (Physical Layer Convergence Procedure) preamble, a PLCP header and a Physical Service Data Unit (PSDU). Each PSDU consists of the MAC header, the frame body (MSDU), and extra bits (Tail/Pad bits) (IEEE Std 802.11b, 1999).

Figure 3 shows the format of an ERP-OFDM PPDU, which is common to the 802.11g PHY standard. ERP-OFDM is the most often implemented PPDU in the 802.11g standard, and supports data rates of 6, 9, 12, 18, 24, 36, 48, and 54 Mbps. The ERP-OFDM PPDU has three parts: Preamble, Header, and Data Field. The PLCP preamble is carefully designed to enable synchronization. IEEE 802.11g typically uses the ERP-OFDM mode for the PLCP format. With the ERP-OFDM preamble, it takes just 16μs to train the receiver after first detecting a signal on the RF medium with respect to the 144μs for IEEE 802.11b. Failure in frame detection and/or synchronization results in a physical layer (PHY) error. The ERP-OFDM header carries the essential information needed by the receiver to properly decode the rest of the frame. The Data field consists of the Service subfield, PSDU, Tail subfield, and Pad Bits subfield. The Service subfield consists of 16 bits, with the first 7 bits as zeros to synchronize the receiver descrambler. The remaining 9 bits are reserved for future use and set to all 0s. As part of the Data field, the Service subfield is transmitted at the rate specified in the Signal field's Rate subfield.

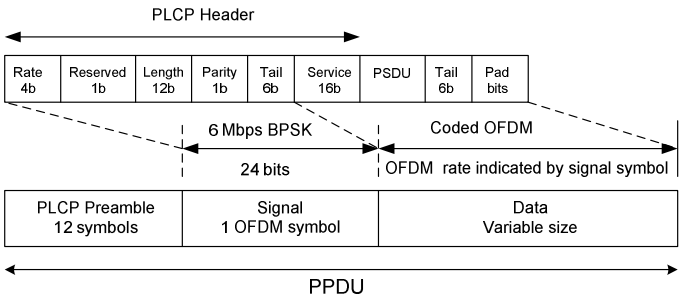

Figure 3: ERP-OFDM PPDU Framing.

In the 802.11g standard extends the use of the DSSS PHY by specifying an optional PPDU type consisting of the same DSSS preamble and header, but at the cost of accepting an ERP-OFDM PPDU as its PSDU. The IEEE calls this new PPDU type DSSS-OFDM. Both long and short preambles are supported with DSSS-OFDM, and no protection mechanisms are required by DSSS-OFDM stations when operating with DSSS stations present in the BSA. Figure 4 illustrates the construction of both long and short preamble formats for DSSS-OFDM PPDUs. The preamble and header transmission rates apply to DSSS-OFDM as with DSSS.

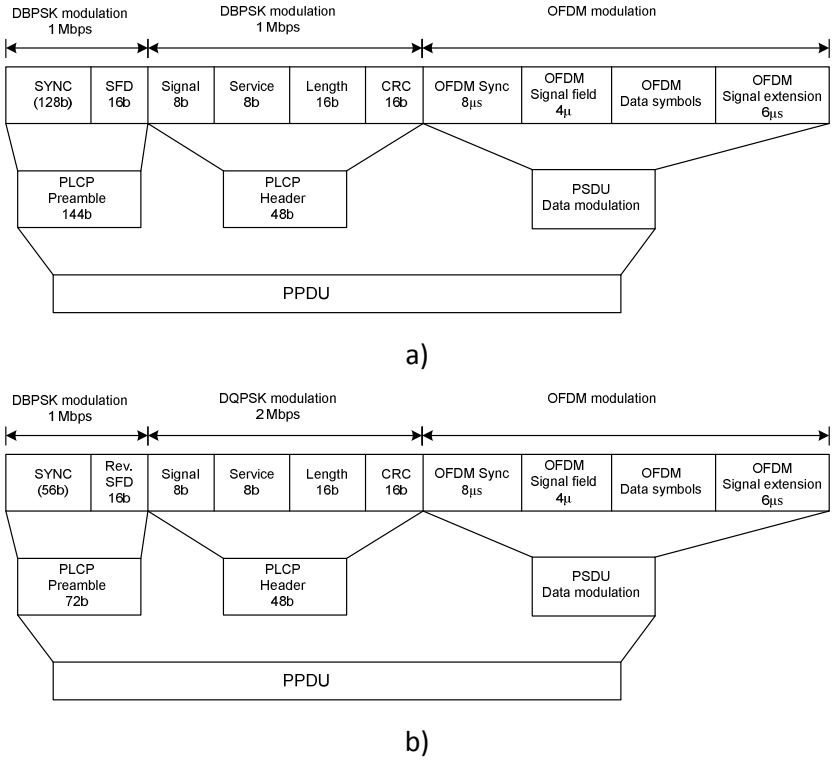

Figure 4: DSSS-OFDM PPDU Framing, a) long preamble, b) short preamble.

1.2.4 MEDIUM ACCESS CONTROL OF 802.11G

The IEEE 802.11g standard builds on the MAC protocol specifications defined for legacy 802.11 networks (IEEE Std 802.11, 1999; IEEE Std 802.11a, 1999; IEEE Std 802.11b,1999). In the 802.11 standard there are two different schemes that can be used in the medium control access.

When the Point Coordination Function (PCF) is employed, the access point controls access to the medium by assigning time slots to each station. The Distributed Coordination Function (DCF) on the other hand, needs no central coordinator. Because the PCF scheme is an optional access method of the 802.11 standard, only the functionality of the DCF will be described in this section. In addition, DCF defines a randomized access mechanism, which is based on the CSMA/CA (Carrier Sense Multiple Access/Collision Avoidance).

DCF constitutes the fundamental access mechanism of the original IEEE 802.11 standard. According to DCF, a WLAN station must sense the medium before initiating the transmission of a packet. If the medium is sensed idle for a time interval greater than a Distributed InterFrame Space (DIFS), the station transmits the packet. Otherwise, the transmission is deferred and a backoff process begins. Specifically, the station initializes and begins decreasing a timer called a backoff counter. As soon as the backoff counter expires, the station is authorized to access the medium. The initial value of the backoff counter is defined as the backoff window, which is a random time interval uniformly distributed in the range of [0,CWmin − 1]. The parameter CWmin constitutes the minimum contention window and is doubled after each unsuccessful retransmission attempt up to a maximum value CWmax called the maximum contention window. Note that in the special case where the time elapsed between the last packet transmission and the current packet transmission is less than a DIFS, the station is obliged to execute the backoff process for the first transmission attempt. Given that collision detection is not possible in a WLAN environment, an Acknowledgement (ACK) is used to notify the sending station that the transmitted frame has been successfully received. The transmission of the acknowledgement is initiated at a time interval equal to the Short InterFrame Space (SIFS) after the end of the reception of the transmitted frame. The above described DCF mechanism is depicted in Figure 5a.

In addition to the basic access mechanism, the IEEE 802.11 standard includes a protection mechanism for dealing with the hidden terminal problem (Kim et al., 2006). This mechanism is based on the exchange of two short control frames: a Request To Send (RTS) frame that is sent by a potential transmitter to the receiver and a Clear To Send (CTS) frame that is sent from the receiver in response to the RTS frame. The RTS and CTS frames include a duration field that specifies the time interval necessary to completely transmit the data frame and the related acknowledgement. Other stations can hear either the sender (RTS frame), or the receiver (CTS frame), in order to refrain from transmitting until the data frame transmission is completed. The effectiveness of the RTS/CTS mechanism depends upon the length of the packet being protected. Usually, a hybrid approach is used, where only packets with a size greater than a threshold called RTS Threshold are transmitted with the RTS/CTS mechanism. The operation of the RTS/CTS protection mechanism is depicted in Figure 5b. Moreover, this protection mechanism is used to improve the performance in 802.11b/g, and it communicates to 802.11g stations utilizing the CCK scheme. Other protection mechanism used in 802.11g is the CTS-to-self. In this protection mechanism, a station sends a CTS message when it desires to send data, even though there is no RTS message received. Both of these mechanisms are designed to help reduce collisions.

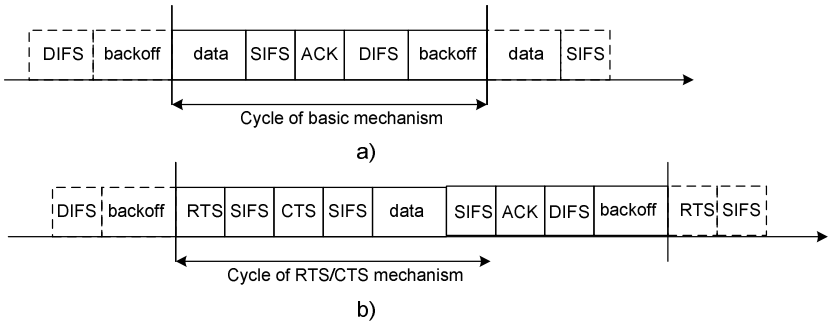

Figure 5: Access Mechanisms: a) basic, b) RTS/CTS.

1.2.5 ANALYSIS OF THROUGHPUT AND DELAY

Throughput is defined as the ratio of successfully transmitted payload from of one node to another in a specified amount of time,

$$S = \frac{\text{successfully transmitted payload}}{\text{transmission time (delay)}}. \quad (1)$$

Taking into account the time diagram of the access mechanism (see Figure 5), we can derive the theoretical maximum achievable throughput (TMT) and minimum delay for IEEE 802.11g in both g-only and b/g modes. The following calculations assume ideal conditions for packet transmission, i.e., there is no packet loss.

In a scenario where the system is composed of both 802.11b and 802.11g stations (hybrid system), 802.11g can operate in an 802.11g ERP-OFDM scheme and ERP-CCK/DSSS (both mandatory). The 802.11b system, however, can only detect packets transmitted by ERP-CCK/DSSS, making it necessary to use a protection mechanism, such as that described in Section 1.2.4. Therefore, the throughput is calculated as:

- ERP-CCK/DSS scheme:

$$S = \frac{MSDU_{size}}{T_{data} + T_{SIFS} + T_{ACK} + T_{DIFS} + T_{backoff}}, \quad (2)$$

and

- ERP-OFDM scheme:

$$S = \frac{MSDU_{size}}{T_{RTS} + T_{SIFS} + T_{CTS} + T_{SIFS} + T_{data} + T_{SIFS} + T_{ACK} + T_{DIFS} + T_{backoff}}. \quad (3)$$

where:

TRTS is RTS time, TSIFS is SIFS time, TDIFS is DIFS time, Tdata is transmission time for the payload, TACK is ACK transmission time, and $T_{backoff} = \frac{CW_{\min} T_{slot}}{2}$, where CWmin is the minimum backoff window size, and Tslot is a specified time slot.

If the system is composed only of 802.11g stations, it does not require the protection scheme. Therefore, the throughput is calculated according to equation 2.

1.2.6 IEEE 802.16 WMAN ARCHITECTURE

WiMAX (Worldwide Interoperability for Microwave Access) is an emerging wireless communication system that is expected to provide high data rate communications in metropolitan area networks (MANs). In the past few years, the IEEE 802.16 working group has developed a number of standards for WiMAX. The first standard was published in 2001, which supports communications in the 10-66 GHz frequency band. In 2003, IEEE 802.16a was introduced to provide additional physical layer specifications for the 2-11 GHz frequency band. These two standards were further revised in 2004 (IEEE 802.16-2004). Recently, IEEE 802.16e has also been approved as the official standard for mobile applications.

Physical Layer

In the physical (PHY) layer, IEEE 802.16 supports four PHY specifications for the licensed bands. These four specifications are Wireless-MAN-SC (single carrier), -SCa, -OFDM, (orthogonal frequency – division multiplexing), and –OFDMA (orthogonal frequency –division

multiple access). In addition, the standard also supports different PHY specifications (-SCa, -OFDM, and –OFDMA) for the unlicensed bands: wireless high-speed unlicensed MAN (WirelessHUMAN). Most PHYs are designed for non-line-of-sight (NLOS) operation in frequency bands below 11 GHz, except –SC, which is for operation in the 10-66 GHz frequency band. To support multiple subscribers, IEEE 802.16 supports both time-division duplex (TDD) and frequency-division duplex (FDD) operations.
The mobile version of IEEE 80.16 also supports the following features to enhance the performance of the wireless system: 1) multiple input, multiple output (MIMO) technique such as transmit/receive diversity multiplexing, 2) multiple antennas schemes can also be used to increase the performance by increasing the transmitted data rates through spatial multiplexing, and 3) adaptive modulation and coding (AMC) is used to better match instantaneous channel and interference conditions.

Medium Access Control Sub-layer

In the medium access control (MAC) layer, IEEE 802.16 supports two modes: point-to-multipoint (PMP) and mesh. The former organizes nodes into a cellular-like structure consisting of a base station (BS) and subscriber stations (SSs). The channels are divided into uplink (from SS to BS) and downlink (from BS to SS), and both uplink and downlink channels are shared among the SSs. PMP mode requires all SSs to be within the transmission range and clear line of sight (LOS) of the BS. On the other hand, in mesh mode, an ad hoc network can be formed with all nodes acting as relay routers in addition to their sender and receiver roles, although there may still be nodes that serve as BSs and provide backhaul connectivity.

In PMP, requests for resource allocations and data transmissions from SSs to the BS are carried in an uplink (UL) frame. Transmissions from the BS to SSs are carried by a downlink (DL) frame. A typical signaling frame for TDD includes a UL-frame (see Figure 6a) and a DL-frame (see Figure. 6b) using a single channel frequency as illustrated in Figure 6c. In FDD, these frames are transmitted at the same time using different channel frequencies as illustrated in Figure 6d.

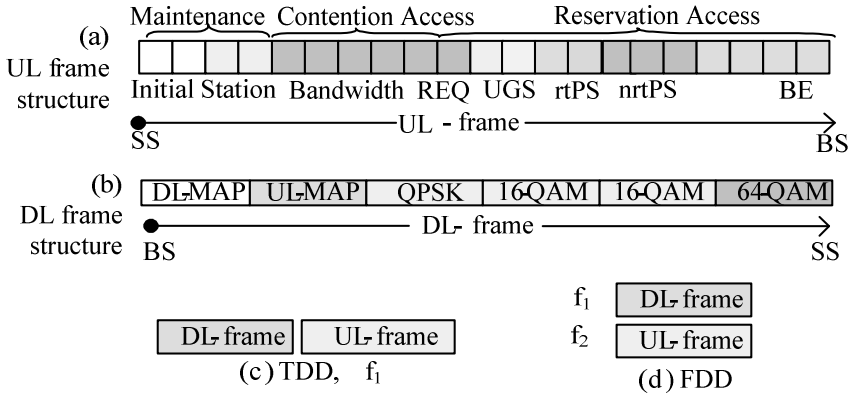

Figure 6: Frame structure for TDD and FDD access.

The IEEE 802.16 MAC protocol regulates uplink (UL) channel access using Time Division Multiple Access (TDMA). Upon entering the BWA network, each Subscriber Station (SS) has to go throughout the initialization process setup, described as follows:
Subscriber stations need to synchronize with a downlink channel (DL-Ch) and an uplink channel (UL-ch). When a SS has tuned to a DL-ch, it gets the frame structure of the UL-ch, called a UL-MAP frame. Then the ranging procedure is performed, where the round-trip delay and power calibration are determined for each SS, so that SS transmissions are aligned to the

correct mini-slot boundary. Following this, the SS negotiates basic capabilities with the BS. This is the phase where the SS and the BS exchange their supported parameters. Next, the SS should use the Privacy Key Management (PKM) protocol to receive authentication from the BS. Then the SS performs the registration process by establishing a security association that allows the SS to enter the network. The next step is to establish IP connectivity. The BS uses the DHCP mechanisms to obtain an IP address for the SS and any other parameters needed to establish IP connectivity. Then, the SS establishes the time of the day, which is required for time-stamping logged events and key management. In the next step, the SS transfers control parameters via TFTP, such as boot information, QoS parameters, fragmentation, and packing, among others. The last step is to set up connections for pre-provisioned service flows belonging to the SS.

After the initialization process is completed, a SS can create one or more connections over which its data is transmitted to and from the BS. SSs contend for transmission opportunities using the contention access period (or contention block) of the current UL-frame. The BS collects these requests and determines the number of slots (grant size) that each SS will be allowed to transmit in the next UL-frame, using a UL_MAP sub-frame, as shown in Figure 6a. The UL-MAP frame contains Information Elements (IE), which describe the maintenance, contention or reservation access of the UL-frame. The UL-MAP is broadcasted in the DL channel by the BS in each DL-Frame. After receiving the UL-MAP, an SS can transmit data in the predefined reserved slots indicated in the IE. These reserved slots are transmission opportunities assigned by a scheduling algorithm using the following QoS service agreements.

Unsolicited Grant Service (UGS): This service supports real-time service flows that generate fixed-size data packets on a periodic basis (CBR-like services), such as T1/E1, VoIP or videoconferencing. At the beginning of the connection setup, an SS provides the BS its service requirements, such as grant size, grant inter-arrival time, tolerated grant jitter and Poll bit. The UGS service also includes Activity Detection (AD) to examine the flow state. If the state is inactive, then the UGS-AD Service sets the Poll bit to 1 and periodically provides a unicast transmission opportunity, in which an SS can request the BS reestablish its UGS service, thus saving bandwidth.

Real-Time Polling Service (rtPS): This service supports real-time service flows that generate variable size data packets on a periodic basis (VBR-like services), such as MPEG video streams. The rtPS service offers periodic transmission opportunity, which meets the flow's real-time needs and allow the SS to specify the size of the desired channel reservation. A SS should indicate its requirements to the BS at the beginning of the session, such as polling interval and tolerated poll jitter.

Non Real-Time Polling Service (nrtPS): This type of service is similar to rtPS, however polling will typically occur at a much lower rate and may not necessarily be periodic. This applies to applications that have no requirement for a real time service but may need an assured high level of bandwidth. An example of this may be bulk data transfer (via FTP) or an Internet gaming application. The parameters required for this service are the polling interval, minimum and maximum sustained data rate.

Best Effort (BE): This kind of service is for standard Internet traffic, where no throughput or delay guarantees are provided.

The IEEE 802.16 MAC protocol can identify the type of service flow required by an SS using the following fields of the IEEE 802.16 protocol stack: source or destination MAC address, EtherType, source and destination IP address or network, IP protocol type, source or destination port number, IP type of service bits and any combination thereof. A simple example of how a classification might be used would be to match VoIP traffic from a particular source IP address

and UDP port and to direct that traffic into a dynamically created service flow that has a QoS parameter set that provides a UGS mode of data transmission.
Once the service flows have been identified, the BS uses two modes of operation to allocate grants: 1) Grants per Connection (GPC) and Grants per Subscriber Station (GPSS). In the first case, the BS grants bandwidth explicitly to each connection, whereas in the second case the bandwidth is granted to all the connections belonging to the SS. The latter case (GPSS) allows smaller uplink maps and allows more intelligent SSs to make last moment decisions and perhaps utilize the bandwidth differently than it was originally granted by the BS. This may be useful for real-time applications that require a faster response time from the system.

1.2.7 ANALYSIS OF THROUGHPUT AND DELAY FOR IEEE 802.16

This analysis only considers a best effort (BE) service. We start by describing the sequence of actions that take place when a subscriber station (SS) makes use of a BE service for data transfer. When a SS is active, (let us say SS_x), it forms a continuous loop with the sequence of actions depicted in Figure 7. When a packet arrives from an upper layer protocol, the SS_x waits for the next UL-MAP containing a contention period. Then, the SS_x randomly chooses one of the available contention minislots and transmits a bandwidth request (REQ) indicating the packet length. If some other SS (let us say SS_y) selects the same contention minislot, a collision occurs and the subscriber stations (SS_x and SS_y) receive neither a grant nor an acknowledgement (ACK) in the following UL-MAP. Thus, the SS_x retransmits its REQ until it is successfully transmitted. Upon successful reception of a REQ from the SS_x, the BS converts the packet size to a number of minislots that should be reserved in subsequent UL-frames. In case the REQ from the SS_x does not fit in the next UL-frame, the BS sends a null grant to the SS_x in order to acknowledge the REQ.
Modeling of such events can be carried out by breaking down a single packet transmission in its delay components. Let us denote by i the time delay, measured in minislots, from the time a packet arrives from the upper layers until the beginning of the contention block where SS_x transmits its REQ. Let c represent the total time in minislots spent during contention, which starts with the beginning of the contention block where the SS_x transmits the first REQ, until SS_x receives an ACK (i.e., a null grant in the IEEE 802.16 protocol). Let us define by w the time in minislots that the scheduler takes in order to grant the REQ of the SS_x. It is measured from the ACK reception to the grant reception at the SS_x. At the BS, the scheduler serves REQs using a FIFO discipline. If the REQ from the SS_x cannot be granted in the next UL-frame, it waits until previous REQs from other SSs are served. Note that in case a REQ can be immediately served, instead of returning an ACK, the BS returns a grant indicating the number of minislots that were reserved. In this case, reception of such a grant also signals the end of the contention time c and therefore w is zero.
Finally, let us denote by x the delay component that represents the actual number of minislots spent during packet transmission from the SS_x. Figure 7 depicts the relation between the events described above and the delay components of the model. Therefore, the time to transmit a single packet (t) can be directly obtained by adding all delay components, i.e., $t = i + c + w + x$. By taking expectation on both sides of this equation we obtain:

$$\bar{t} = \bar{i} + \bar{c} + \bar{w} + \bar{x}. \tag{4}$$

From these parameters, the normalized network throughput (γ) of the UL channel can be computed as the fraction of minislots actually spent in data transmission per station, scaled to the total number of SSs (N), thus:

$$\gamma = N\bar{x} / \bar{t}\,. \tag{5}$$

The aim of this paper is to provide a method to compute this metric. The notation used in this

derivation is presented in Table I.

Regarding Eq. (5), it is necessary to compute $\bar{x}$ and $\bar{t}$. The mean delay for packet transmission in minislots (i.e., $\bar{x}$) can be directly obtained from the packet size distribution, taking into consideration that minislots can be 2, 4, 8, 16, 32 or 64 bytes. Thus

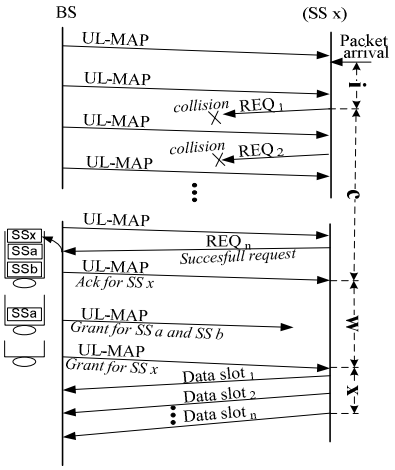

Figure 7: Access delay components.

Table I. IEEE 802.16 MAC Model Notation

Symbol	Definition
C	Size of the contention block in a UL-frame
R	Size of the reservation period in a UL-frame
M	Total size of a UL-frame, $M=C+R$
i	Initial delay
c	Contention delay to transmit a REQ successfully
w	Time to grant a REQ for a SS
x	Time spent in a packet transmission
t	Total time in a transmission cycle, $t = i + c + w + x$
$\bar{i}$, $\bar{c}$, $\bar{w}$, $\bar{x}$, $\bar{t}$	Expectations of i, c, w, x, and t, respectively
P_{SC}	Probability of a successful contention in a UL-frame
n	Number of SSs contending in the current UL-frame
s	Number of SSs that transmitted a REQ successfully in the current UL-frame
$\bar{n}$, $\bar{s}$	Expectations of n and s, respectively
$\bar{b}$	Expected number of contention periods per cycle, $\bar{t}$
N	Maximum number of active SSs
P_C	Probability that a SS contends in a contention period
P_S	Probability of a successful contention in a minislot
$\bar{d}$	Available transmission minislots for a SS per cycle
γ	System throughput

$$\bar{x} = \left\lceil \frac{\bar{m} + MAC\_OV + PHY\_OV}{slot\_size} \right\rceil \tag{6}$$

where $\bar{m}$ is the mean packet size at the LLC layer, *MAC_OV* is the MAC overhead of the IEEE 802.16 protocol (the default value for *MAC_OV* is 6 byes). The overhead at the physical layer, *PHY_OV,* depends on the coding techniques involved (see (IEEE 802.16-2004) Chapter 8, for further information on coding rates and modulation techniques).

Computation of $\bar{t}$ implies calculating other delay components as described below. Estimating the mean initial delay $\bar{i}$ has to consider the following three delay factors. First, packet arrival from an upper layer protocol may occur anywhere within the current UL-frame, thus the SS must wait for the next available contention block before transmitting a REQ. The mean value for this delay can be approximated by *M*/2 minislots, where *M* is the total length of the UL-frame. Second, the SS has to wait a complete frame of size *M* minislots in order to transmit a REQ in the available contention block of the next UL-frame. Third, once the REQ is received, the BS may grant this REQ anywhere in the following UL-frame, which can also be approximately by *M*/2 minislots. Thus the initial delay, can be approximated as

$$\bar{i} \cong 2M. \tag{7}$$

Whereas computation of $\bar{x}$ and $\bar{i}$ is straightforward, computation of $\bar{c}$ and $\bar{w}$ is far more complicated. This procedure is described in the following sections.

Computation of the contention delay

For simplicity, we assume that the number of failed contentions that a SS needs to succeed follows a geometric distribution. Thus, given the probability of a successful contention in a contention block (P_{SC}), the mean number of minislots used for contention $\bar{c}$ would be given by

$$\bar{c} = C + M\,\frac{(1 - P_{SC})}{P_{SC}} \tag{8}$$

where C is the size of the contention block and M is the total length of a UL-frame (both measured in minislots).
Let $\bar{n}$ and $\bar{s}$ be the expected number of the total and successful contenders in a contention block, respectively. It is clear that the probability P_{SC} can be estimated as

$$P_{SC} = \frac{\bar{s}}{\bar{n}}. \tag{9}$$

Le us now turn our attention to the estimation of $\bar{n}$ and $\bar{s}$. Let us denote by P_C the probability that a SS decides to contend in a contention block. Therefore, the expected number of contenders in a contention block is given by

$$\bar{n} = NP_C \tag{10}$$

and the number of successful contenders per contention block is

$$\bar{s} = (NP_C)P_{SC}. \tag{11}$$

Note that there are $\bar{t}$ minislots per transmission cycle and one contention block every M minislots. Therefore, the mean number of contention blocks ($\bar{b}$) per transmission cycle is given by

$$\bar{b} = \frac{\bar{t}}{M}. \tag{12}$$

Let us assume that the system is operating in steady state. Under this assumption, each active SS gets a chance to transmit every $\bar{t}$ minislots and parameter $\bar{s}$ can be estimated dividing the total number of SS among the mean number of contention blocks per transmission cycle as follows

$$\bar{s} = \frac{N}{\bar{b}}. \tag{13}$$

Substituting (12) in (13) we obtain

$$\bar{s} = \frac{MN}{\bar{t}}. \tag{14}$$

From (10) and (14) in (9) we can obtain

$$P_C = \frac{M}{P_{SC}\bar{t}}. \tag{15}$$

Let us define the probability of successful contention in an arbitrary slot P_S as the probability that, from the mean number of contenders in a contention block $\bar{n}$, only *one* contends in a minislot (packet capture is not possible),

$$P_S = \binom{\bar{n}}{1}\frac{1}{C}\left(1 - \frac{1}{C}\right)^{\bar{n}-1}. \tag{16}$$

Therefore, parameter $\bar{s}$ can be computed as

$$\bar{s} = CP_S . \tag{17}$$

From (17) and (11) P_{SC} can be computed as

$$P_{SC} = \frac{CP_S}{NP_C} . \tag{18}$$

Note that computation of $\bar{c}$ in (8) implies computation of P_{SC} which in turn depends on computation of P_C and P_S as indicated by (18). At this point, it is fair to mention that the authors in (Chite & Daigle, 2003) made use of these three probabilities in their analysis of IP-based services over GPRS networks. Although P_C and P_{SC} are computed here in the same way, the fact that we do not consider packet capture allows us to compute P_S in a fundamentally different way. Computation of this probability as defined by (16) is not equivalent to the method presented in (Chite & Daigle, 2003). This difference allows us to go one step further.

The authors in (Chite & Daigle, 2003) make use of the previously derived probabilities in order to iteratively compute P_{SC}. Although our model and theirs differ in several ways, we also made use of this procedure with good results. The procedure starts by assuming that $\bar{w}$ is known and providing an initial estimate for P_{SC}. Then, from (8), (4), (15) and (16) we compute P_C and P_S. These values are used in (18) in order to obtain the following value for P_{SC}. With this value the process can be repeated starting from (8). This loop can be ended when the difference between two consecutive values for P_{SC} is below a certain threshold. The final value for P_{SC} allows us to compute the value for the contention delay $\bar{c}$ using (8). Further adjustments on $\bar{w}$ would be needed if the assumed value for $\bar{w}$ does not satisfy all system conditions.

In what follows we derive the equation that represents the procedure just described. Let us identify with subindex n the n-th iteration. Thus, (8) and (4) become $\bar{c}_n = C + M\left(1 - P_{SC_n} / P_{SC_n}\right)$ and $\bar{t}_n = \bar{i} + \bar{c}_n + \bar{w} + \bar{x}$, respectively. From these equations, we have

$$\bar{t}_n = \bar{i} + C + M\left(\frac{1 - P_{SC_n}}{P_{SCn}}\right) + \bar{w} + \bar{x} . \tag{17}$$

From (15) we know that $P_{Cn} = M / \left(P_{SC_n} \bar{t}_n\right)$ which combined with (19) yields,

$$P_{C_n} = \frac{1}{\beta P_{SC_n} + 1} \tag{20}$$

where $\beta = \left(\left(\bar{i} + C + \bar{w} + \bar{x}\right)/M\right) - 1$.

From (10) and (20) the estimated mean number of users at the n-th iteration is

$$\bar{n}_n = \frac{1}{\beta P_{SC_n} + 1} N . \tag{21}$$

From (16) and (21) the estimated value of the probability of successful contention in an arbitrary slot at the n-th iteration is

$$P_{S_n} = \frac{N}{\beta P_{SC_n} + 1} \left(\frac{1}{C}\right) \left(1 - \frac{1}{C}\right)^{\frac{N}{\beta P_{SC_n} + 1} - 1} . \tag{22}$$

Finally, from (20), (22) and (18) the difference equation that can be used to obtain the value of P_{SC} is

$$P_{SC\,n+1} = \left(1 - \frac{1}{C}\right)^{\frac{N}{\beta P_{SC_n} + 1} - 1} . \tag{23}$$

In summary, given $\overline{w}$ and an initial estimate for P_{SC}, we iterate (23) until a consistent value for P_{SC} is obtained. With this value the contention delay $\overline{c}$ can be computed using (8). The algorithm implied by (23) is very easy to implement and it is much simpler than the one presented in [14].

Computation of the waiting delay

Recall that the value of $\overline{w}$ was assumed in the previously described procedure. It is necessary to determine whether this value needs to be adjusted or not. To this end, let us compute the mean number of available transmission minislots for each SS in an average transmission cycle. Let us denote this amount by $\overline{d}$. It is given by

$$\overline{d} = \frac{\overline{t} - C\overline{b}}{N}. \tag{24}$$

In addition, we know that the average number of transmission minislots required per SS is $\overline{x}$. Therefore, the minimum number of transmission minislots in a transmission cycle must be at least of $N\overline{x}$. If $\overline{d} < N\overline{x}$, we propose to increase $\overline{w}$ according to

$$\overline{w}_{m+1} = \overline{w}_m + 1. \tag{25}$$

and compute $\overline{c}$ again according to the procedure described in the previous section. If $\overline{d} \geq \overline{x}$, we can take the corresponding value of $\overline{w}$ and proceed to calculate the system throughput.
We could have updated $\overline{w}$ using larger steps as suggested in (Chite & Daigle, 2003), however increasing this value by one as shown in (25) provides good accuracy and the time to carry out this computations turns out to be negligible in a conventional computer.

Performance Analysis

The performance of the IEEE 802.16 system was analyzed using analytical and simulation models. A detailed simulation model of the IEEE 802.16 MAC protocol was implemented using OPNET Package v. 11 (Simulation software, 2009). For the simulation model, we used a network of 100 SSs distributed randomly in a cell with a radio of 5 km. Also, the minislot size was set to 16 bytes and the UL MAP describes M=450 minislots (=2ms) in the UL-frame. This corresponds to a 28.8 Mbps UL channel. All SSs used Best Effort technique for grant service. The traffic model used by active SSs was Constant Bit Rate (CBR) service created from packets of 300 bytes at the MAC layer with a constant interarrival time of value $\overline{t}$. When these packets are coded at the physical layer of the IEEE 802.16 system, they become 21 minislots ($\overline{x}$=21) using a codeword of 255 bytes, Reed Solomon parity of 10 bytes, preamble of 6 bytes and guard band of 4 bytes. In the simulation model, the size of the backoff window of the EBA was not allowed to grow. It was set at a fixed value according to the size of contention block used in the corresponding simulation (i.e., 30, 51, and 72 minislots). For the analytical model, we used an initial delay of $\overline{w}_0 = 1$ minislot and $P_{SC\,0} = 0.01$.
We examined the throughput as a function of the number of active subscriber stations. Figure 8 shows the maximum system throughput as a function of the number of backlogged SSs. This figure includes the results of the analytical and simulation models with the number of contention minislots as a parameter.
For a small number of contention minislots per UL-frame, (i.e., C = 30 minislots), we observed that the maximum system throughput achieved with both models is approximately 52% of the channel capacity; this corresponds to a network with 40 SSs. This throughput is limited by the

excessive number of collisions reported in each UL-frame. With 40 SSs, the average number of grants served per UL-frame was of 11.6 of a total of $(M\text{-}C)/\bar{x}) = 21$ grants. The rest of the UL-frame was wasted, since just a few REQ could arrive to the BS due to collisions.
By increasing C to 51 minislots, the average number of grants served by a UL-frame increased considerably to 17, which nearly achieves 90% of system throughput when there are between 60 and 70 SSs. However, when there is a large number of SSs in the network, (i.e., more than 80 SSs) the system throughput cannot be maintained due to the large number of collisions reported.

With C = 72 minislots, the system throughput can be sustained even in very large networks, however the maximum system throughput is just over 80% of channel capacity.
For the three values of C shown in Fig. 8, we observed that simulation results were in good agreement with analytical results. The maximum deviation from our simulation model was less than 3%.

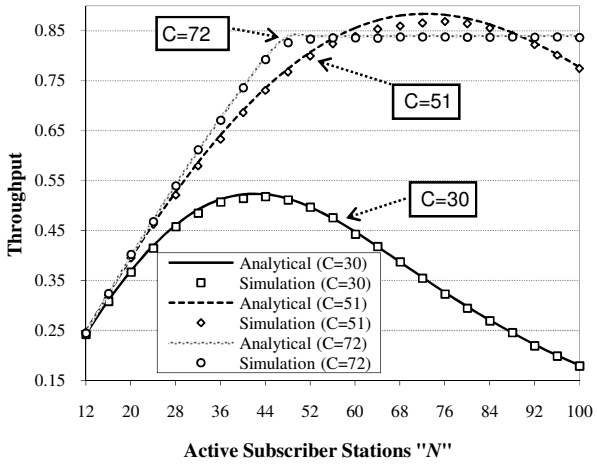

Figure 8: Performance analysis of IEEE 802.16 based Network.

2. SIMULATION MODEL FOR VANET

2.1 INITIALIZATION PROCESS OF THE MESH NODE

The initialization process at the mesh node carries out three principal phases: (1) the creation of the broadcast flow, (2) the neighbor discovery process and finally (3) the establishment of individual unicast flows for each of the neighbors, as show in Figure 9.

The generation of two broadcast flows, each with its corresponding CID (connection identifier) is one of the first processes carried out at the moment mesh nodes begin to interact. One of these flows is utilized to transmit the broadcast information generated in the upper layers of the mesh node (data), while the second flow is the control broadcast that sends information to the MAC layer. The discovery process and neighbor node localization is modeled by the simulator (software) which registers objects based on the existing distances between each one of the nodes. For each neighbor node discovered, a unicast Hello message is sent to the upper data layers, which have the ability to administer the connection and accept the request, forwarding a response to the corresponding CID and establishing one of the points for the unicast flow connection. If the node responds affirmatively, it stores the request and establishes the other link point identified by a connection (CID) with the neighbor. In this way, it completes the other end point of the data flow. It is important to mention that, at some moment, the establishment of connections to the mesh node itself may be necessary. For this reason, mesh nodes should

generate the identification and the connection and forward them, if possible, to the requesting node.

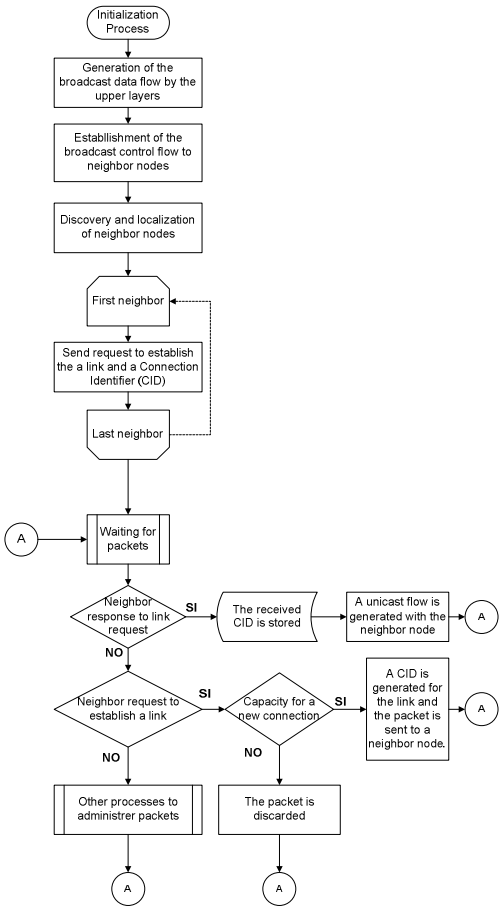

Figure 9: Initialization process of the mesh mode.

IEEE 802.11g (WiFi) and IEEE 802.16e (WiMAX) standards, respectively, include ad hoc and mesh topology in their specifications. However, to the best of our knowledge, there are no simulation results for Vehicular Ad Hoc Networks (VANETs) with mesh-WiMAX technology. In this work, we propose a new simulation model for VANETs with a mesh architecture.

The advantage of our model is that it does not require a Base Station (BS), which is a compulsory element for point-to-multipoint architectures. Our simulation model has been implemented in OPNET Modeler (Simulation software, 2009) as shown in the Figure 10. OPNET Modeler is an important network simulator that can be used to design and study communication networks, devices, protocols and applications. In addition, our simulation model is compatible with the PMP architecture.

The simulation model requires a new parameter to determine the direction of the communication. This is realized at the physical layer and is called a mesh link. The communication direction for the PMP architecture consists of a downlink and uplink; this is one important difference between mesh and the PMP architectures. Table II, describes the main parameters utilized in the simulation model.

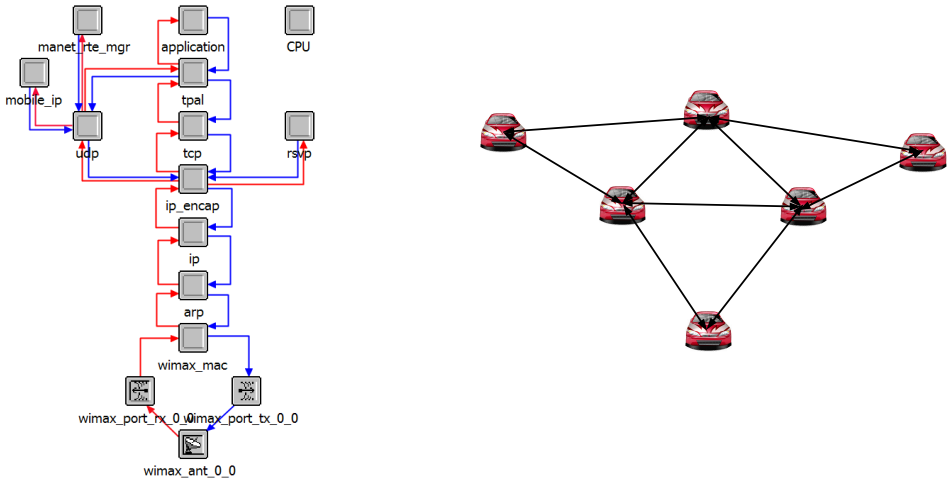

Figure 10: Simulation model for mesh architecture.

Parameters	Value
Antenna Gain (dBi)	-1 dB
Maximum Number of SS Nodes	10
Minimum Power Density (dBm/subchannel)	-90
Maximum Power Density (dBm/subchannel)	-60
CDMA Codes: Number of Initial Ranging Codes	8
CDMA Codes: Number of HO Ranging Codes	8
CDMA Codes: Number of Periodic Ranging Codes	8
CDMA Codes: Number of Bandwidth Request Codes	8
Back Off Parameters: Ranging Back Off Start	2
Back Off Parameters: Ranging Back Off End	4
Back Off Parameters: Bandwidth Request Back Off Start	2
Back Off Parameters: Bandwidth Request Back Off End	4
Neighbor Advertisement Interval (frames)	10
Neighborhood ID	0
Scanning Interval Definitions: Scanning Threshold (dB)	0.0
Scanning Interval Definitions: Scan Duration (N) (Frames)	5
Scanning Interval Definitions: Interleaving Interval (P) (Frames)	240
Scanning Interval Definitions: Scan Interaction (T)	10
Scanning Interval Definitions: Start Frame (M) (Frames)	5
Handover Parameters: Resource Retain Time (100 milliseconds)	2 (200 milliseconds)
Channel Quality Averaging Parameter	4/16
Distance Neighbors	1000 mts.
MAC Address	Auto Assigned
Maximum Transmission Power (W)	0.01
Mesh Role	Uncoordinated
PHY Profile	Wireless OFDMA 20 MHz
PHY Profile Type	OFDM
Multipath Chanel Model	ITU Pedestrian A
Path loss Model	Free Space

Terrain Type (Suburban Fixed)	Terrain Type A
Shadow Fading Standard Deviation	Disable Shadow fading
Ranging Power Step (mW)	0.25
Timers: T3 (ms)	50
Timers: T4 (ms)	10
Contention Ranging Retries	16

Table II: Simulation parameters for the mesh WiMAX model

3. SIMULATION SCENARIOS

The simulation scenarios were implemented in OPNET Modeler. The scenarios simulate and compare two emerging wireless technologies, IEEE 802.11g and IEEE 802.16e, in a Vehicular Ad hoc Network (VANET) of 20, 40, 60, 80 and 100 vehicular nodes uniformly distributed within a 200m x 200m area (Figure 10). We employed the Orthogonal Frequency Division Multiplexing (OFDM) at the physical layer and the Carrier Sense Multiple Access with Collision Avoidance (CSMA/CA) at the MAC layer for IEEE 802.11g (Scenario 1). Scenario 2 employs OFDM in the physical layer and Time Division Multiple Access (TDMA) in the MAC layer, as specified by IEEE 802.16e. Both scenarios consider one broadcast transmitter and 20, 40, 60, 80 and 100 broadcast receivers under a constant transmission range of 1000m (Figure 11). The simulation scenarios have a constant bit rate (CBR) for data flow and a uniform payload size of 512 bytes. The simulation parameters are listed in Tables III and IV.

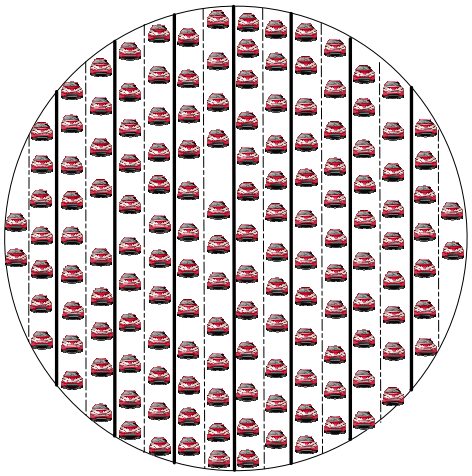

Figure 11: Simulation Scenario for WiFi and WiMAX models.

The Cluster-Based Location Routing Algorithm (LORA-CBF) was employed for single-hop inter-vehicle communications (Santos et al., 2005), (Santos et al., 2009).
Each vehicle detects neighboring vehicles to which it has a direct link. To accomplish this, each vehicle periodically broadcasts a Hello message containing its address and status. These control messages are transmitted in broadcast mode and are received by all one-hop neighbors. Data packets start at 100 seconds and are resent every second until the end of the simulation.

Parameter	Value
Simulation area	200 m x 200 m
Total nodes	20, 40, 60, 80 and 100

Channel capacity	54 Mbps
MAC protocol	IEEE 802.11g
Packet flows	Constant bit rate (CBR)
Packet payload	512 bytes
Physical layer	OFDM
Simulation time	200 seconds
Frequency	2.4 GHz

Table III: Simulation parameters for scenario 1.

Parameter	Value
Simulation area	200 m x 200 m
Total nodes	20, 40, 60, 80 and 100
Channel capacity	54 Mbps
MAC protocol	IEEE 802.16e
Packet flows	Constant bit rate (CBR)
Packet payload	512 bytes
Physical layer	OFDM
Simulation time	200 seconds
Frequency	3.5 GHZ

Table IV: Simulation parameters for scenario 2.

4. RESULTS OBTAINED BY SIMULATIONS

Figure 12 shows the delay for scenarios 1 and 2. IEEE 802.11g technology does not suffer any impact in delay because of the LORA-CBF algorithm. However, IEEE 802.16e technology suffers a minimal impact in terms of delay; For 20 vehicles, the delay is almost 7.0 ms, for 40 vehicles 5.5 ms, for 60 vehicles 4.8 ms, for 80 vehicles 4.4 and for 100 vehicles 4.2 ms. The results of these two simulations permit us to infer that the delay for IEEE 802.16e technology is approximately 4 ms.

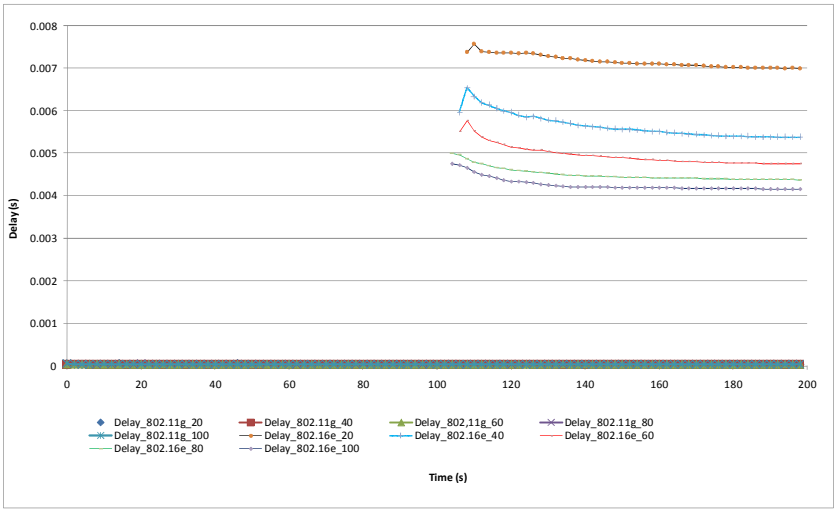

Figure 12: Delay for scenarios 1 and 2.

Figure 13 shows the load for scenarios 1 and 2. There is no impact in load for IEEE 802.11g technology due to the LORA-CBF algorithm. However, for IEEE 802.16e technology, there is an impact in terms of load; for 20 vehicles, the load is almost 100,000 b/s, for 40 vehicles 230,000 b/s, for 60 vehicles 500,000 b/s, for 80 vehicles 900,000 b/s and for 100 vehicles 1.3 Mb

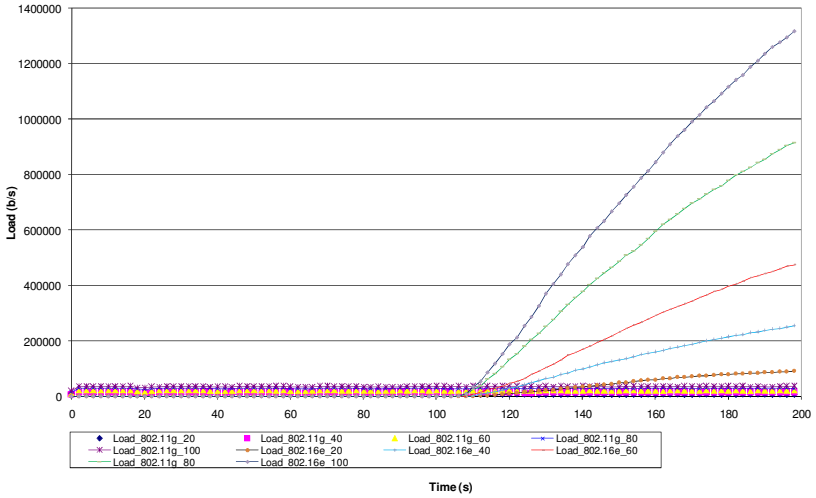

Figure 13: Load for scenarios 1 and 2.

Figure 14 shows the throughput for scenarios 1 and 2. Again, there is no impact in throughput for IEEE 802.11g technology due to the LORA-CBF algorithm. However, for IEEE 802.16e technology, there is an impact in terms of throughput; for 20 vehicles the throughput is less than 5 Mb/s, for 40 vehicles is less than 10 Mb/s, for 60 vehicles is approximately 20 Mb/s, for 80 vehicles approximately 50 Mb/s and for 100 vehicles approximately 90 Mb/s.

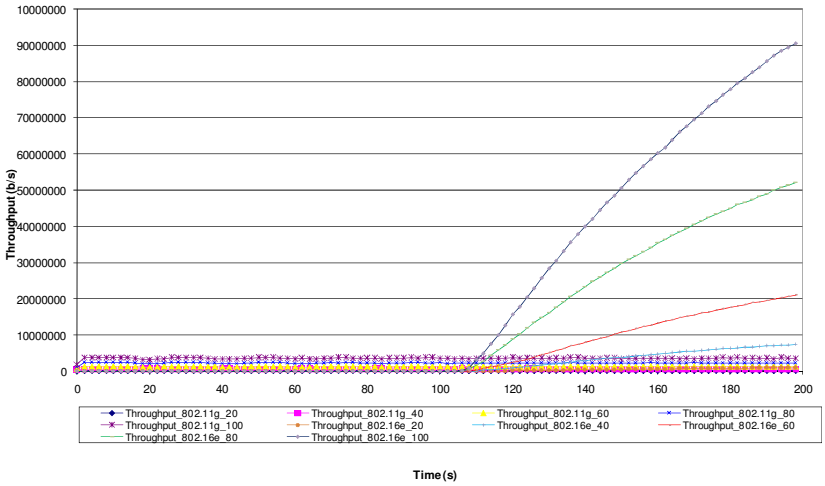

Figure 14: Throughput for scenarios 1 and 2.

5. CONCLUSIONS

This chapter showed the results of two prominent technologies used for single-hop inter-vehicular communications (WiFi and WiMAX). We simulated similar scenarios employing both technologies and applied a Location Based Routing Algorithm with Cluster-Based Flooding (LORA-CBF) for broadcast data transmission. In addition, we considered a hierarchical vehicular organization that acts as a cluster-head with its corresponding member nodes. The simulation scenarios consisted of five different node sizes of 20, 40, 60, 80 and 100 vehicles, respectively. We provided preliminary results in terms of delay, load and throughput for single-hop inter-vehicle communications. Results show that WiMAX requires several processes before the node can begin its data transmission. These processes produce some delay, which impacts the previously mentioned metrics. However, WiMAX outperforms WiFi in terms of throughput. Another important advantage is that the proposed model is suitable for a mesh topology in a WiMAX network and is compatible with the PMP architecture.

REFERENCES

Chite, V. A., Daigle, J. N. (2003). Performance of IP-Based Services over GPRS. IEEE Transactions on Computers, vol. 52, No. 6, pp. 727-741.

Da Chen, Z., Kung, H.-T., & Vlah, D. (2001). Ad Hoc Relay Wireless Networks over Moving Vehicles on Highways. Proceedings in International Conference on Mobile Computing and Networking, pp. 247-250.

Füßler, H., Mauve, M., Hartenstein, H., Käsemann, M., & Vollmer, D. (2003). MobiCom Poster: Location-Based Routing for Vehicular Ad-Hoc Networks. Proceedings in ACM SIGMOBILE Mobile Computing and Communication Review, volume 7, issue 1, pp. 47-49.

Johnson, D., Maltz, D., & Hu, Y.–C. (2007). The Dynamic Source Routing Protocol (DSR) for Mobile Ad Hoc Networks for IPv4. http://www.ietf.org/rfc/rfc4728.txt. Request for Comments (Work in Progress).

IEEE Std. 802.11. (1999). Part 11: Wireless LAN Medium Access Control (MAC) and Physical Layer (PHY) Specifications.

IEEE Std. 802.11a. (1999). Part 11: Wireless LAN Medium Access Control (MAC) and Physical Layer (PHY) Specifications: High-speed Physical Layer in the 5GHz Band.

IEEE Std. 802.11b. (1999). Part 11: Wireless LAN Medium Access Control (MAC) and Physical Layer (PHY) Specifications: Higher-speed Physical Layer Extension in the 2.4GHz Band.

IEEE Std. 802.11g. (2003) Part 11: Wireless LAN Medium Access Control (MAC) and Physical Layer (PHY) Specifications- Amendment 4: Further Higher Data Rate Extension in the 2.4GHz Band.

IEEE 802.16-2004 (2004). IEEE Standard for Local and Metropolitan Area Networks - Part 16: Air Interface for Fixed Broadband Wireless Access Systems.

Karp, B., & Kung, H.-T. (2000). Greedy Perimeter Stateless Routing for Wireless Networks. Proceedings of the 6th ACM International Conference on Mobile Computing and Networking, pp. 243-254.

Kim, Y., Yu, J., Choi, S., and Jang, K. (2006). A novel hidden station detection mechanism in IEEE 802.11 WLAN. *IEEE Communications Letters*, 10(8), 608-610.

Kosh, T., Schwingenschlögl, C., & Ai, L. (2002). Information Dissemination in Multihop Inter-vehicle Networks – Adapting the Ad-hoc On-demand Distance Vector Routing Protocol (AODV). Proceedings in the 5th IEEE International Conference on Intelligent Transportation Systems, pp. 685-690.

Li, J., Jannotti, J., De Couto, D., Karger, D., & Morris, R. (2000). A Scalable Location Service for Geographic Ad Hoc Routing. Proceedings of the 6th ACM International Conference on Mobile Computing and Networking, pp. 120-130.

Lochert, C., Füßler, H., Hartenstein, H., Hermann, D., Tian, J., & Mauve, M. (2003). A Routing Strategy for Vehicular Ad Hoc Networks in City Environments. Proceedings of the IEEE Intelligent Vehicles Symposium, pp. 156-161.

Morris, R., Jannotti, J., Kaashock, F., Li, J., & Decouto, D. (2000). A Scalable Ad Hoc Wireless Network System. Proceedings of the 9th workshop on ACM SIGOPS European Workshop: beyond the PC: new challenges for the operating system, pp. 61-65.

O'Hara, B.; & Petrick, A. (1999). The IEEE 802.11 Handbook: A Designer's Companion. Standards Information Network. IEEE Press.

Perkins, C., Belding-Royer, E., & Das, S. (2003). Ad hoc On-Demand Distance Vector (AODV) Routing. http://www.ietf.org/rfc/rfc3561.txt. Request for Comments (Work in Progress).

Raúl Aquino-Santos, Víctor Rangel-Licea, Miguel A. García-Ruiz, Apolinar González-Potes, Omar Álvarez-Cárdenas, Arthur Edwards-Block, Margarita G. Mayoral-Baldivia, Sara Sandoval-Carrillo. (2009). Chapter title: Inter-vehicular Communications using Wireless Ad Hoc Networks. Book Title: Automotive Informatics and Communicative Systems: Principals in Vehicular Networks and Data Exchange. Ed. Guo, Huaqun. IGI Global, pp. 120-138. ISBN: 978-1-60566-338-8.

Santos, R. A., Edwards, A., Edwards, R. M. and Seed, N. L. (2005) "Performance evaluation of routing protocols in vehicular ad-hoc networks". International Journal of Ad Hoc and Ubiquitous Computing. Vol.1, Nos. 1/2, pp. 80-91. ISSN: 1743-8233.

Simulation software. Last access, on May 1, 2009. http://www.opnet.com/solutions/network_rd/modeler.html

Szczypiorski, K., and Lubacz, J. (2008). Saturation throughput analysis of IEEE 802.11g (ERP-OFDM) networks. Telecommunication Systems, 38(1-2), 45-52.

Toh, C. -K. (2002). Ad Hoc Mobile Wireless Networks: Protocols and Systems. Prentice-Hall International, Inc.

Vassis, D., Kormentzas, G., Rouskas, A., and Maglogiannis, I. (2005). The 802.11g Standard for High Data Rate WLANs. IEEE Networks, 19(3), 21-26.